Effects of nano-sized carborundum particles and amino silane coupling agent on the cure reaction kinetics of DGEBA/EMI-2,4 system

Tianle Zhou*, Mingyuan Gu, Yanping Jin, Junxiang Wang

State Key Laboratory of MMCs, Shanghai Jiao Tong University, Shanghai 200030, China

Abstract

The influence of nano-sized carborundum (nano-SiC) particles and amino silane coupling agent on the curing kinetics of bisphenol-A glycidol ether epoxy resin (DGEBA) initiated with 2-ethyl-4-methylimidazole (EMI-2,4) was studied by means of non-isothermal differential scanning calorimetry (DSC). Besides decreasing the heat of reaction ΔH, the presence of nano-SiC particles results in delayed cure reactions, which is also manifested by the increased values of exothermic peak temperature T_p and cure reaction activation energy E of the filled systems. Meanwhile, the amino silane coupling agent could increase ΔH, and decrease slightly the degree of delayed cure reactions caused by nano-SiC particles, and thereby decreasing T_p of the filled systems. The presence of nano-SiC particles prevents from the occurrence of vitrification, so does the amino silane coupling agent when the nano-SiC particle content is low ($\lesssim 15$ wt%). As the nano-SiC particle content is high ($\gtrsim 15$ wt%), the presence of amino silane coupling agent promotes the occurrence of vitrification. Besides E, the presence of nano-SiC particles could increase the overall order of reaction $m+n$ and the frequency factor A, meanwhile, the amino silane coupling agent decreases these three parameters.
© 2005 Elsevier Ltd. All rights reserved.

Keywords: Cure reaction kinetics; DGEBA/EMI-2,4 system; Nano-SiC

1. Introduction

With the advancement in nanoscience and nanotechnology, there is increasing interest in polymer nanocomposites, both in scientific research and for engineering applications. As the filler size decreases into the nano level, high surface area of the nanofillers results in their high surface activity, and the volume fraction of the interaction region in the nanocomposites increases with the increasing interface area of the polymer and nanofillers. These become the basis for potentially tremendous changes in the nanocomposite properties, such as the rheological, mechanical, dielectric and thermal mechanical properties, etc. [1,2]. Therefore, nanocomposites have become promising materials in many applications, and studies on the properties of the nanocomposites have been developed rapidly, but there is a lack of study on the curing kinetics of the nanocomposites.

Owing to the exceptionally low coefficient of thermal expansion (CTE) and the high thermal conductivity (TC) of SiC, the SiC filled composite materials have gained great interest to reduce the CTE and improve the TC of the polymer composites. In this paper, nano-SiC particles with average particle size of 50 nm were used with DGEBA/EMI-2,4 system as the base system.

In this work, nano-SiC particles were pretreated with amino silane coupling agent, which was employed to enhance the compatibility between the nano-SiC particles and the epoxy matrix, as well as preventing from the agglomerations of the nano-SiC particles. One end of the amino silane-coupling agent formed a hydrogen bond with the nano-SiC particles, therefore, there were several coupling agent molecular layers on the surface of the nano-SiC particles after the surface treatment. Then the epoxy system was blended with these surface modified nano-SiC particles, the other end of the amino silane coupling agent would enter in the epoxy macromolecule by means of chemical bond to form an interface layer between

Table 1
Compositions of tested specimens (by weight)

System	DGEBA	EMI-2,4	Amino silane coupling agent	Nano-SiC particles
A1	100	6	0	0
A2	100	6	0	5
A3	100	6	0.5	5
A4	100	6	1	10
A5	100	6	2	20
A6	100	6	3	20
A7	100	6	4	20

the nano-SiC particle and epoxy matrix during the subsequent cure reaction. Consequently, the formation of a cross-linked nano-SiC particles/resin network can be achieved.

Since the nano-SiC particles and the amino silane coupling agent play important roles in the polymer composite system, this paper attempts to provide an in-depth understanding in the effect of them on the curing characteristics of the polymer composite system and, therefore, to provide guidance for choosing the proper set of processing parameters. A particular emphasis is given to the study of the vitrification phenomena and theoretical work has been elaborated to explain the influence of the nano-SiC particles and the amino silane-coupling agent on the vitrification phenomena of the polymer composite system. This study is part of a wider investigation on high performance nanocomposites for more demanding applications, such as in microelectronics applications, etc.

2. Experimental

Epoxy resin used in this work was a nominally difunctional epoxy resin, Epon 828, supplied by Shanghai Resin Co. Epon 828 is, basically, DGEBA with the epoxy value of 0.48–0.52 mol/100 g. The curing agent utilized was EMI-2,4 supplied by Beijing Chemical Reagent Co. The nano-SiC particles with average particle size of 50 nm were obtained from Karl Co. and used as-received or treated with the amino silane coupling agent, γ-aminopropyl-triethoxysilane (A1100), from Shanghai Chemical Reagent Co. Other agents utilized were analytically pure grade and were supplied by Beijing Chemical Reagent Co.

Surface treatment of nano-SiC particles using amino silane involved (i) making a silane-absolute ethyl alcohol solution at a selected concentration, (ii) adding nano-SiC particles to the solution and stirring with a magnetic stirrer for 30 min, (iii) heating at 333–353 K for 30 min, (iv) rinsing with alcohol by filtration, and (v) drying at 383 K for 12 h.

The specimens with the compositions listed in Table 1 were prepared at ambient temperature. The base polymer formulation was prepared by mixing DGEBA and EMI-2,4 with a weight ratio of 100:6 for 15 min. A specified quantity

of nano-SiC particles, pretreated with different concentration of amino silane coupling agent, was added into the base polymer and the mixture was dispersed by sonication for 30 min since nano-SiC particles are known to agglomerate easily due to their high surface area and hydrophilic surface property.

A sample of approximately 10 mg was weighed accurately into an aluminum DSC sample pan and then covered with an aluminum lid. The entire operation was carried out in a dry chamber. The exotherm was measured under a nitrogen flow rate of 10 ml min^{-1} with a Perkin–Elmer DSC-7 system. The DSC was calibrated with high purity indium; α-Al$_2$O$_3$ was used as the reference material. The exotherm baseline was corrected via data on the empty aluminum pan. Dynamic DSC measurements were performed at different heating rates of 10, 15, 20 K/min over a temperature range of 303 to 623 K. The reaction was considered to be complete when the rate curve leveled off to a baseline. The cured sample was left in the DSC cell and cooled to room temperature. Then the cured sample was scanned at 20 K/min to determine the T_g of the reacted product. The initial temperature of the heat flow step of the second diagram was taken to be the T_g.

The viscosity of the nanocomposites at room temperature was studied using a stress rheometer (TA Instruments, ARES9A) in a steady flow mode. A cone-and-plate geometry was used. A freshly prepared liquid uncured sample was dispensed on the plate before the run and the experiments were conducted under stepped shear rate from 0.01 to 100 s^{-1}.

3. Results and discussion

The curing mechanism of DGEBA/EMI-2,4 system involves two stages consisting of the adduct and etherification reactions [3–5]. The adducts were believed to be the catalyst that initiated the etherification reactions which cross-link the epoxy resins and determine the final properties of the network. Previous work showed that the adduct formation was necessary prior to the etherification reaction. Thus, low EMI-2,4 concentrations can be used to analyze the etherification reactions by suppressing the adduct formation [4].The objective criterion of meeting this specification is that the molar heat of the reaction ΔH approaches a constant. It is shown that the variation amplitude of ΔH is small when the concentration of EMI-2,4 is between 3 and 10 wt% (gram mass of EMI-2,4 per 100 g mass of DGEBA), as the cure reaction is incomplete when the content of EMI-2,4 is below 3 wt% [6]. In this work, the concentration of EMI-2,4 is 6 wt% which falls within the range of 3–10 wt%, that is to say, the heat of reaction for the etherification reaction peak is approximately the total heat of the curing reaction. Furthermore, the heat released during the chemical reaction between the amino silane coupling agent and the epoxy resins is so small
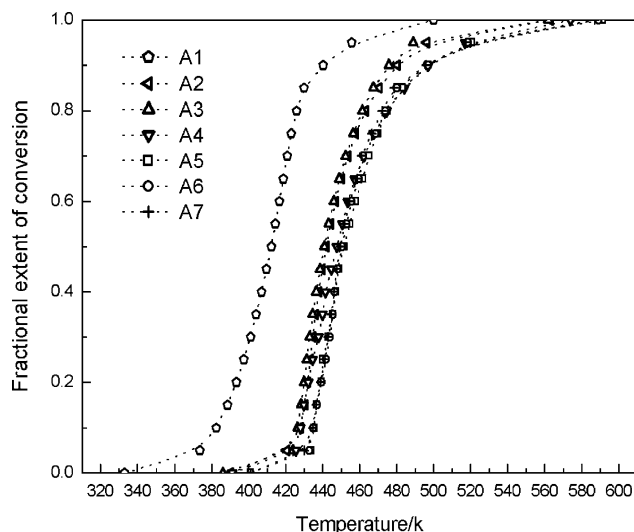
Fig. 1. Advancement of the cure reactions for non-isothermal cure at 20 K/min heating rate of A1–A7 systems. Dotted lines are given only for showing the tendency.
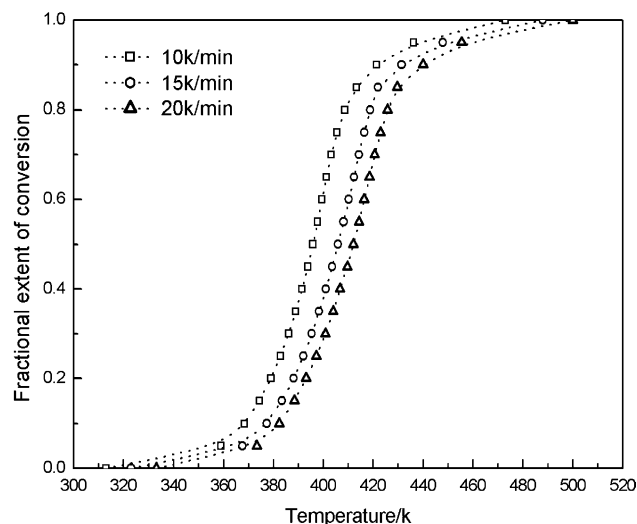

Fig. 2. Advancement of the cure reactions for non-isothermal cure at different heating rates of A1 system. Dotted lines are given only for showing the tendency.

compared with the heat of the curing reaction that it can be safely negligible. Thus, in this work, a single reaction (i.e. the etherification reaction) dominates the cure process. Therefore, ΔH can be considered as a constant over the whole cure reaction. Then, the rate of the cure reaction is $d\alpha/dt = (dH/dt)/\Delta H$ where dH/dt is the heat flow above the baseline. In other words, the rate of cure reaction is assumed to be proportional to the heat release rate.

In order to obtain the individual influence of the amino silane coupling agent and the nano-SiC particles on the curing rate, the advancement of the cure reaction as a function of temperature was investigated using DSC technique. From a dynamic DSC run, the total area S of the exothermal peak (the region between the exotherm and the baseline) is in direct proportion to the molar heat of the reaction ΔH released during the whole cure reaction. The fractional extent of conversion α at any temperature T can be expressed as:

$$\alpha = \frac{\Delta H_T}{\Delta H} = \frac{S_T}{S} \quad (0 \leq a \leq 1)$$

Table 2
Exothermic peak temperatures and heats of reaction for A1–A7 systems at 10 K/min heating rate and the viscosity of each uncured systems at 1 s^{-1} shear rate

System	Peak temperature T_p (K)	Heat of reaction ΔH (kJ mol^{-1})	Viscosity (Pa s)
A1	399.56	361.78	3.776
A2	421.38	340.53	6.438
A3	419.72	349.71	5.898
A4	421.43	329.52	6.717
A5	423.67	286.30	7.838
A6	422.76	301.79	7.323
A7	422.13	319.16	6.972

where ΔH_T is the heat of reaction of partially cured samples heated up to the temperature T.

A comparison of the curing kinetics, at 20 K/min heating rate, among A1–A7 systems is shown in Fig. 1. A sigmoidal form of the curves, which is indicative of an autocatalytic kinetics of all the studied systems, is observed [7]. That is to say, the addition of nano-SiC particles and amino silane coupling agent does not change the cure reaction mechanism of the resin system. It also can be seen that A2–A7 systems present delayed cure reactions compared with A1 system. Although the effect of the amino silane-coupling agent is hard to decide, the cure inhibition effect caused by nano-SiC particles is quite obvious. For the development of the composites, the cure inhibition effect caused by nano-SiC particles could bring negative effect on the composite process since it needs longer post-cure time.

The possible mechanism for the nano-SiC particles delay the cure reactions of epoxy resin system might be the decrease of propagation reaction speed. When the epoxy resin system contained nano-SiC particles, the content of DGEBA and EMI-2,4 decreased with respect to the corresponding unfilled epoxy resin system, the viscosity increased as well, as shown in Table 2, then led to the decrease of propagation reaction speed and made the gel time of epoxy resin longer [8].

Table 2 also summarizes the heats of reaction ΔH and the exothermic peak temperatures T_p for A1–A7 systems. It also can be seen that the presence of nano-SiC particles and amino silane coupling agent can affect the cure reaction of the epoxy system to some degree. The exothermic peak temperatures are higher while the heats of the cure reaction are smaller in A2–A7 systems than in A1 system. The possible reason for ΔH following the sequence A1 > A3 > A4 > A5 might be the decreasing concentration of DGEBA and EMI-2,4 in the systems, and the phenomenon for ΔH
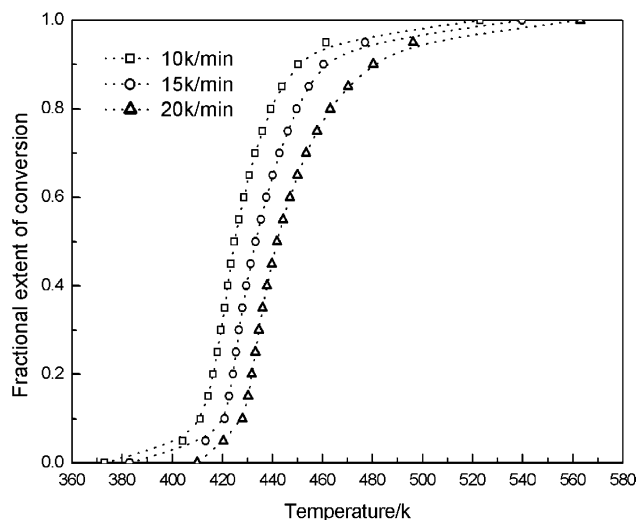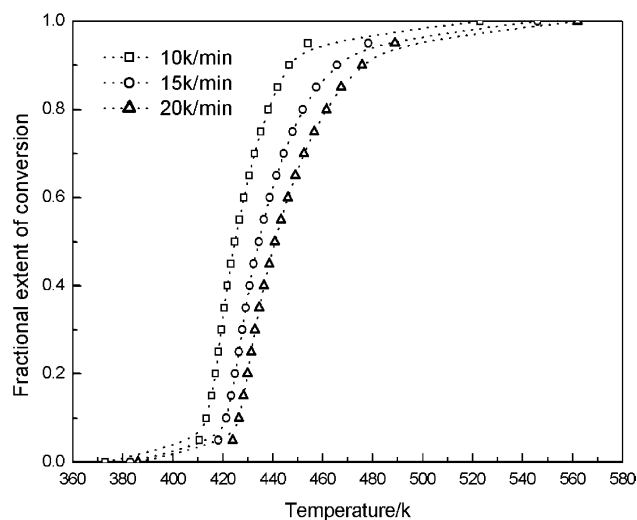
Fig. 3. Advancement of the cure reactions for non-isothermal cure at different heating rates of A2 system. Dotted lines are given only for showing the tendency.

following the sequence A3 > A2 and A7 > A6 > A5 can be attributed to the heat released during the chemical reaction between the amino silane coupling agent and the epoxy resins. Furthermore, the phenomenon for T_p following the sequence A1 < A3 < A4 < A5 also demonstrates that the presence of nano-SiC particles can baffle the occurrence of the cure reaction.

In addition, T_p also follows the sequence A3 < A2 and A7 < A6 < A5. This phenomenon can be due to two reasons. First, the surface treatment on the filler surface would enhance the compatibility between the filler and the epoxy matrix and lower the viscosity of the composite material [9], which can be seen in Table 2, Second, the coupling agent used has amino group (–NH$_2$), which can catalyze the curing reaction of epoxy [10], therefore, it can be deduced

Fig. 4. Advancement of the cure reactions for non-isothermal cure at different heating rates of A3 system. Dotted lines are given only for showing the tendency.
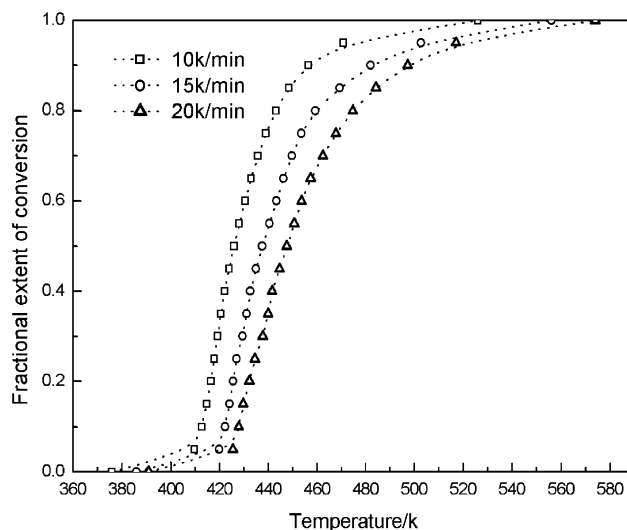

Fig. 5. Advancement of the cure reactions for non-isothermal cure at different heating rates of A4 system. Dotted lines are given only for showing the tendency.

that the amino silane coupling agent can decrease slightly the retarding effect of the cure reactions caused by the nano-SiC particles, thereby decreasing T_p.

In Figs. 2–8, the fractional extent of conversion α vs. temperature T at different heating rates of A1–A7 systems, respectively, is reported. For each formulation all the curves have the same functional form, only shifted a distance along the temperature axis. It follows that all the α vs. temperature curves at different heating rates should be superposable by simply shifting each curve along the temperature axis relative to a curve at an arbitrary reference heating rate by a shift factor, $\phi(\beta) = T_{ref} - T_\beta$, where β is the heating rate.

Figs. 9–15 show the superposed curves of α vs. T for A1–A7 systems taking the curve of 20 K/min heating rate as
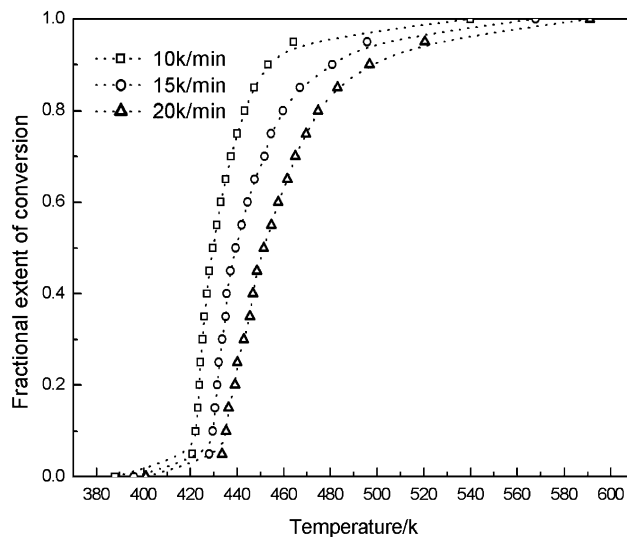

Fig. 6. Advancement of the cure reactions for non-isothermal cure at different heating rates of A5 system. Dotted lines are given only for showing the tendency.
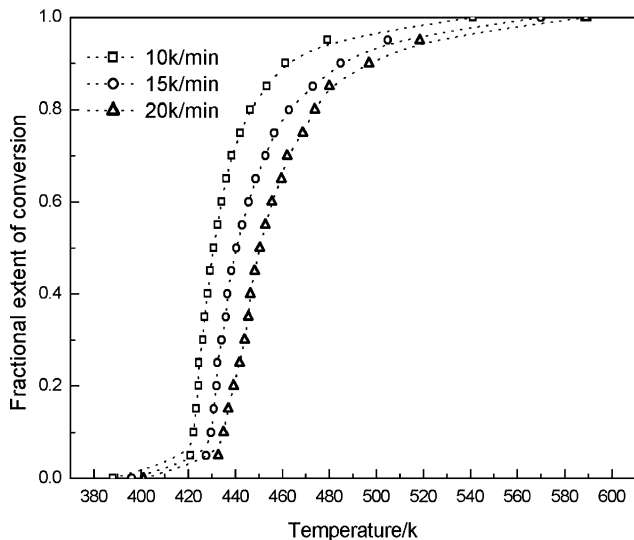
Fig. 7. Advancement of the cure reactions for non-isothermal cure at different heating rates of A6 system. Dotted lines are given only for showing the tendency.

the master curve. The master curve represents the progression of the cure reactions when a material is cured at a reference heating rate.

The phenomenological reaction rate, $d\alpha/dt$, has a general expression:

$$\frac{d\alpha}{dt} = A\, e^{-E/RT} f(\alpha) \qquad (1)$$

where A is the frequency factor, E is the activation energy, $f(\alpha)$ is a function of the fractional extent of conversion α, R is the gas constant and T is the absolute temperature at time t.
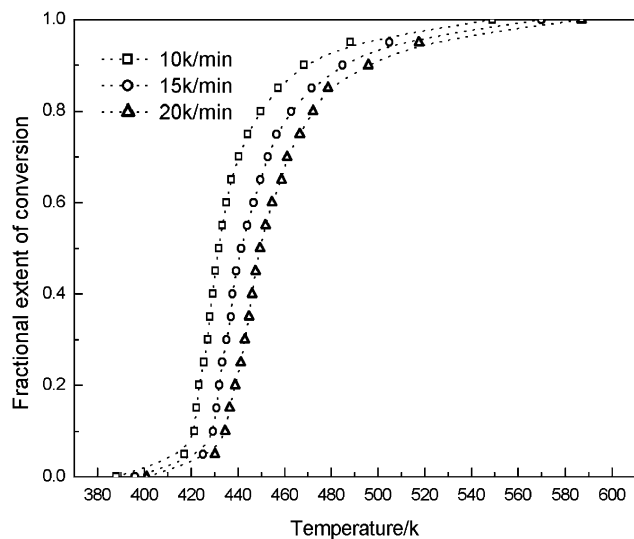

Fig. 8. Advancement of the cure reactions for non-isothermal cure at different heating rates of A7 system. Dotted lines are given only for showing the tendency.
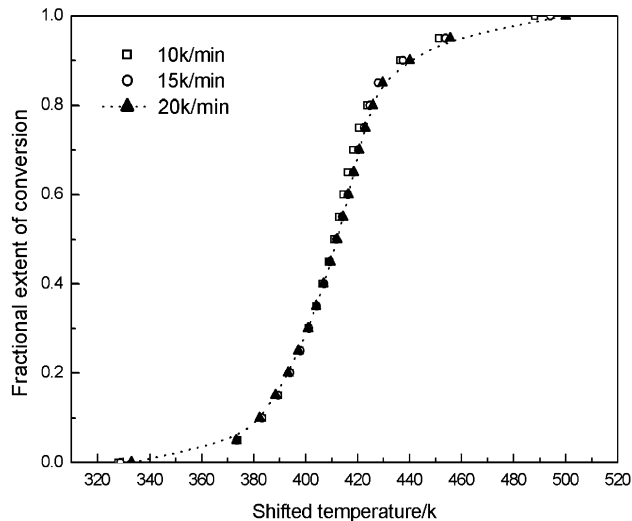

Fig. 9. Superposed curves of α vs. T for A1 system. Dotted line is given only for showing the tendency.

let $T = \beta t$, then $d\alpha/dT$ can be expressed as:

$$\frac{d\alpha}{dT} = A\, e^{-E/RT} \frac{f(\alpha)}{\beta}$$

$$\ln\left(\frac{d\alpha}{dT}\right) - \ln[Af(\alpha)] = -\frac{E}{RT} - \ln\beta \qquad (2)$$

As far as some arbitrary fractional extent of conversion α is concerned, the values of $\ln[Af(\alpha)]$ in the curves at different heating rates are equal while the values of $d\alpha/dT_\beta$, the tangent slope of the point corresponding to the fractional extent of conversion α in the curves at different heating rates, are not always equal to that of the reference curve (i.e. $d\alpha/dT_{ref}$). There are three possibilities: (i) $d\alpha/dT_\beta = d\alpha/dT_{ref}$; (ii) $d\alpha/dT_\beta < d\alpha/dT_{ref}$; (iii) $d\alpha/dT_\beta > d\alpha/dT_{ref}$.
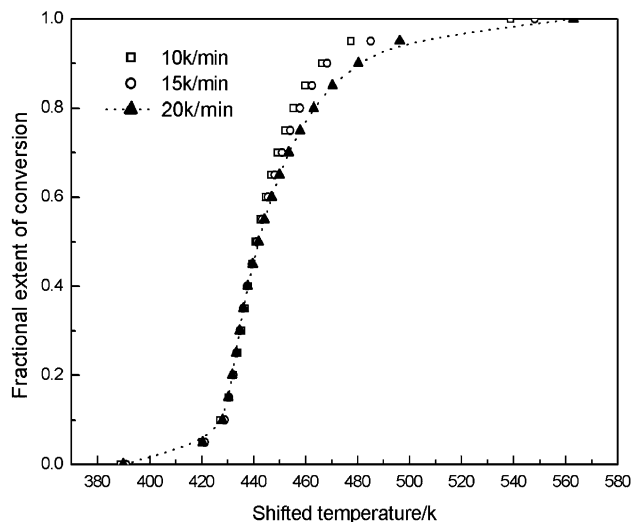

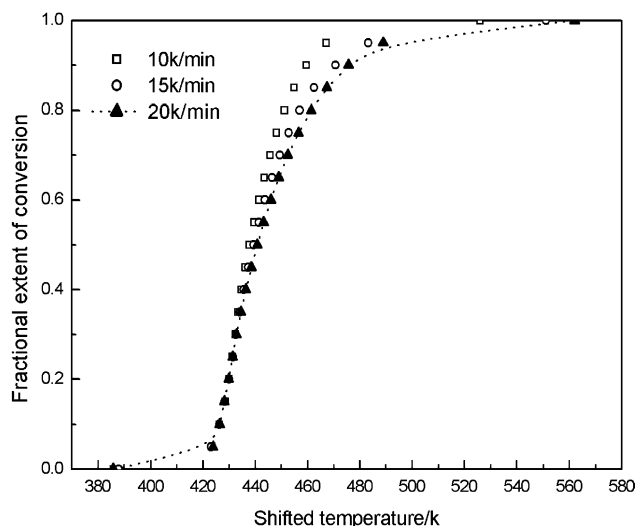Fig. 10. Superposed curves of α vs. T for A2 system. Dotted line is given only for showing the tendency.

Fig. 11. Superposed curves of α vs. T for A3 system. Dotted line is given only for showing the tendency.
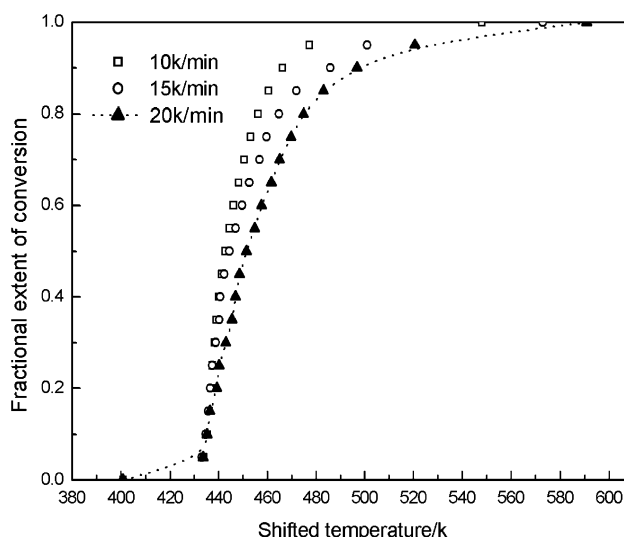

Fig. 13. Superposed curves of α vs. T for A5 system. Dotted line is given only for showing the tendency.

(i) $d\alpha/dT_\beta = d\alpha/dT_{ref}$ then Eq. (2) becomes:

$$-\frac{E}{RT_\beta} - \ln \beta = -\frac{E}{RT_{ref}} - \ln \beta_{ref}$$

$$\frac{1}{T_\beta} - \frac{1}{T_{ref}} = R\left(\frac{\ln(\beta_{ref}/\beta)}{E}\right)$$

thus $T_{ref} - T_\beta$ can be expressed as:

$$T_{ref} - T_\beta = T_\beta T_{ref} R\left(\frac{\ln(\beta_{ref}/\beta)}{E}\right) \qquad (3)$$

The curing curve with 20 K/min heating rate was chosen as the reference curve, then $\beta_{ref}/\beta > 1$ and $T_{ref} - T_\beta > 0$.

Seeing Figs. 2–8, it is obvious that $T_\beta T_{ref}$ will increase as the fractional extent of conversion α increases, then $T_{ref} - T_\beta$ will raise as Eq. (3) shown. The increase of $T_{ref} - T_\beta$ means that $d\alpha/T_\beta > d\alpha/dT_{ref}$ will happen, but this is in contradiction with the original definition that $d\alpha/dT_\beta = d\alpha/dT_{ref}$, so the assumption of $d\alpha/dT_\beta = d\alpha/dT_{ref}$ can not be tenable.

(ii) $d\alpha/dT_\beta < d\alpha/dT_{ref}$ from Eq. (2) we can obtain:

$$\frac{-E}{RT_\beta} - \ln \beta < \frac{-E}{RT_{ref}} - \ln \beta_{ref}$$

$$\frac{1}{T_\beta} - \frac{1}{T_{ref}} > \frac{R \ln(\beta_{ref}/\beta)}{E}$$
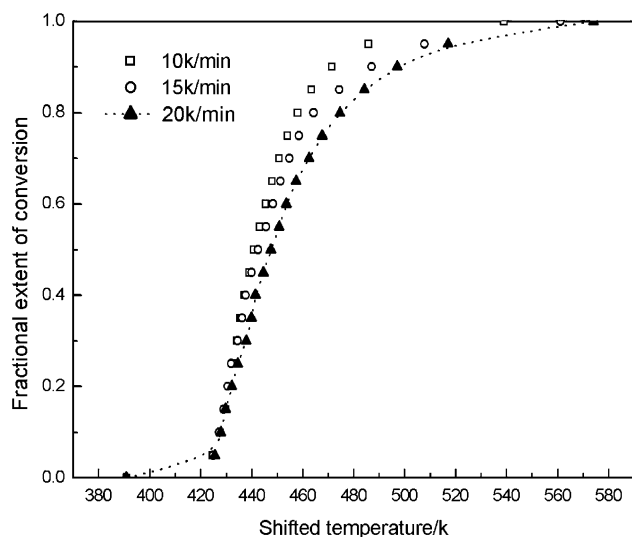

Fig. 12. Superposed curves of α vs. T for A4 system. Dotted line is given only for showing the tendency.
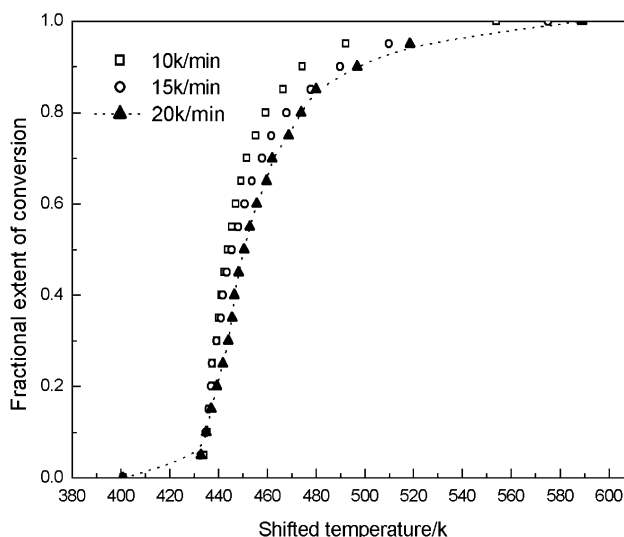

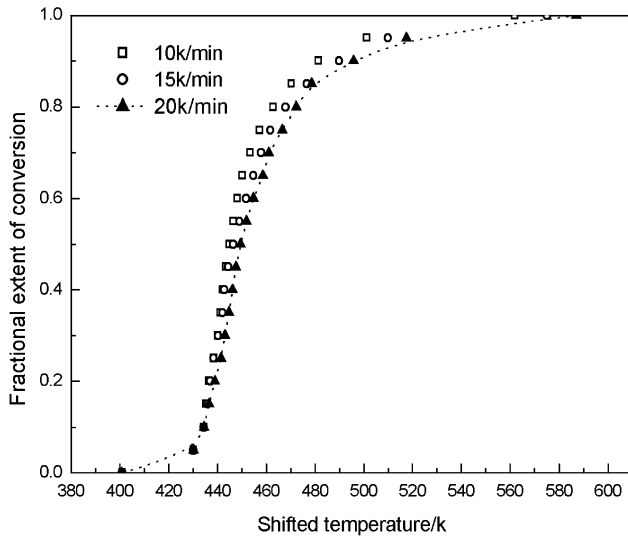Fig. 14. Superposed curves of α vs. T for A6 system. Dotted line is given only for showing the tendency.

Fig. 15. Superposed curves of α vs. T for A7 system. Dotted line is given only for showing the tendency.

then

$$T_{ref} - T_\beta > \frac{T_\beta T_{ref} R \ln(\beta_{ref}/\beta)}{E} \qquad (4)$$

Seeing this in equation, $T_{ref} - T_\beta$ will increase when the fractional extent of conversion α increases. As discussed above, the increase of $T_{ref} - T_\beta$ means that $d\alpha/dT_\beta > d\alpha/dT_{ref}$ which is in contradiction with the original definition that $d\alpha/dT_\beta < d\alpha/dT_{ref}$, so the assumption of $d\alpha/dT_\beta < d\alpha/dT_{ref}$ can not be tenable.

(iii) $d\alpha/dT_\beta > d\alpha/dT_{ref}$, from Eq. (2) we can obtain:

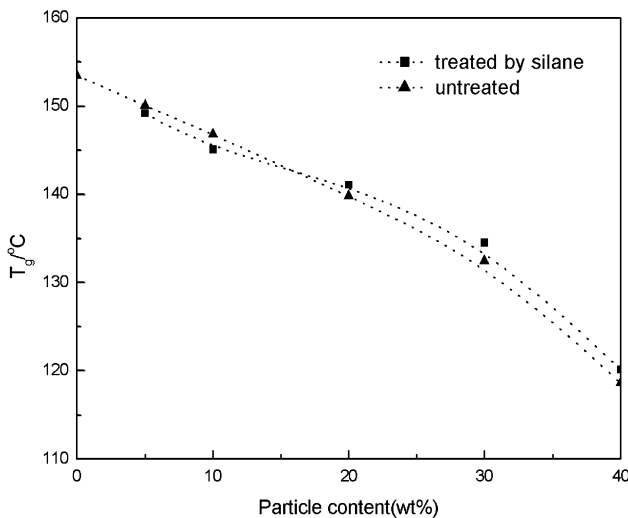$$\frac{-E}{RT_\beta} - \ln \beta > \frac{-E}{RT_{ref}} - \ln \beta_{ref}$$

Fig. 16. Plot of T_g vs. particle content. Amino silane coupling agent: nano-SiC particles = 10:100 by weight. Dotted lines are given only for showing the tendency.

$$\frac{1}{T_\beta} - \frac{1}{T_{ref}} < \frac{R \ln(\beta_{ref}/\beta)}{E}$$

then

$$T_{ref} - T_\beta < \frac{T_\beta T_{ref} R \ln(\beta_{ref}/\beta)}{E} \qquad (5)$$

As discussed above, the assumption of $d\alpha/dT_\beta > d\alpha/dT_{ref}$ means that $T_{ref} - T_\beta$ will increase, and the above in equation means that the increment of $T_{ref} - T_\beta$ can not be greater than $T_\beta T_{ref} R \ln(\beta_{ref}/\beta)/E$, while $T_\beta T_{ref} R \ln(\beta_{ref}/\beta)/E$ itself continuously increases as the fractional extent of conversion α increases. So this inequation is not in contradiction with the original definition.

After the above discussion we can make a conclusion that the above discussed shift factor $\phi(\beta) = T_{ref} - T_\beta$ is not a constant. If the reaction is only kinetically controlled, the curves of the fractional extent of conversion vs. temperature should branch off from the master curve and the shift factor $\phi(\beta) = T_{ref} - T_\beta$ will increase as the fractional extent of conversion α increases.

During the cure reaction, it is possible that the glass transition temperature (T_g) increases over the curing temperature, this phenomenon is called vitrification. When the system vitrifies the cure reaction kinetics becomes diffusion controlled and the values of $d\alpha/dT_\beta$ decrease, i.e. the curves of the fractional extent of conversion vs. temperature do not shift enough from the master curve. Although we do not know the exact degree the curves should shift from the master curve, we can make a qualitative analysis by comparing data from the curves in Figs. 9–15. The superposed curves, reported in Figs. 9–15, indicate that the degree of vitrification phenomena follows the sequences A5 < A4 < A3 < A2 < A1 and A5 < A6 < A7 at any of the heating rates considered. Therefore, the presence of nano-SiC particles prevents from the occurrence of vitrification phenomena, and the influence of the amino silane coupling agent on the vitrification phenomena is complex.

The phenomena can be interpreted by Fig. 16. The T_gs of the nanocomposites are found to decrease with the increasing loading level of nano-SiC particles, treated or untreated with the amino silane coupling agent, thus make it more difficult for T_g to increase over the curing temperature, consequently prevents from the occurrence of vitrification phenomena. Comparing the T_gs of the treated nano-SiC particles filled nanocomposites with those of the untreated nano-SiC particles filled nanocomposites, it can be seen that the addition of the amino silane coupling agent could enhance the T_g depression of the nanocomposites at low nano-SiC particle contents ($\lesssim 15$ wt%), while lessening the T_g depression at higher loading levels ($\gtrsim 15$ wt%) for nano-SiC particles.

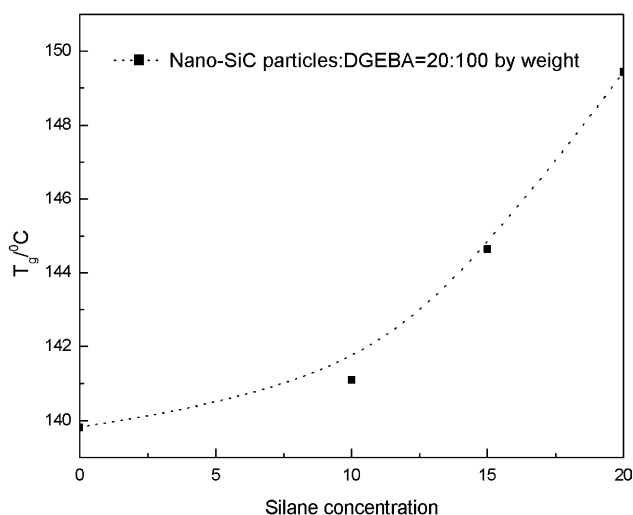The T_g depression deriving from the addition of

Fig. 17. Plot of T_g vs. amino silane coupling agent concentration. Dotted line is given only for showing the tendency.

nano-SiC particles can be due to two reasons [1,2]. First, nano-SiC particles can inhibit the cure reaction as mentioned before, resulting in a lower crosslinking density in the epoxy matrix and, therefore, a lower T_g. Second, nano-SiC particles have much large surface area and interfacial interaction with epoxy matrix. The large particles/resin interface creates extra free volume and, therefore, assists the large-scale segmental motion of the polymer. As a result, T_g of the nanocomposites decreases with increasing filler loading.

When the amino silane coupling agent is introduced into the system, there would, on the one hand, result in a lower T_g. Since the amino group is the end of the amino silane coupling agent which would enter in the epoxy macromolecule by means of chemical bond during the cure reaction, the effect of increased concentration of the amino silane coupling agent was equal to the effect of increased EMI-2,4 concentration in the curing system. As is known that, the use of high levels of EMI-2,4 would increase the concentration of initiating species (the 1:1 adduct) and thus reduce the length of each polymerizing chain (the kinetic chain length). As a result, the reduction of the length of each polymerizing chain would significantly reduce the level of connectivity

Table 3
Cure reaction activation energies system

System	E (kJ mol^{-1})	Correlation coefficient
A1	49.03	0.99548
A2	66.32	0.99038
A3	67.80	0.99292
A4	71.75	0.99988
A5	76.29	0.99947
A6	68.33	0.99934
A7	61.52	0.99963

in the network, lowering the effective crosslinking density and thereby resulting in a lower T_g. On the other hand, the amino silane coupling agent can improve the compatibility between the nano-SiC particles and the epoxy matrix, and thus results in a more 'compact' composite structure and less free volume in polymer [1], therefore, a higher T_g. However, the final result of the amino silane coupling agent on the T_g of the nanocomposites arises from the antagonistic competition of these two factors.

Since the effect for the amino silane coupling agent to improve the compatibility between the nano-SiC particles and the epoxy matrix is more notable at higher nano-SiC particles loading levels, it is understandable for the amino silane coupling agent to lessen the T_g depression at high nano-SiC particle contents ($\gtrsim 15$ wt%). Moreover, for the nanocomposites with high nano-SiC particle content, e.g. 20 wt%, as far as the studied amino silane coupling agent concentrations were considered, the higher amino silane coupling agent concentration, the higher T_g, as shown in Fig. 17, and, therefore, lead to promoted vitrification phenomena. On the other hand, at low nano-SiC particle contents (≤ 15 wt%), the effect of the amino silane coupling agent to improve the compatibility between the nano-SiC particles and the epoxy matrix becomes less important and it is more effective for the amino silane coupling agent to lowering the crosslinking density and thereby resulting in an enhancement in the T_g depression of the nanocomposites, consequently prevents from the occurrence of vitrification phenomena.

Furthermore, the influence of nano-SiC particles and amino silane coupling agent on the curing kinetic parameters of A1–A7 systems was also studied. Ozawa equation, which is concluded to be independent of the order of reaction, is used to calculate the cure reaction activation energy E [11]:

$$\frac{d(-\ln \beta)}{d(1/T_p)} = \frac{1.052E}{R}$$

The value of E can be determined from the slope of the plot of $-\ln \beta$ vs. $1/T_p$.

As discussed above, the studied systems follow autocatalytic kinetics, then $f(\alpha)$ has a generalized expression:

$$f(\alpha) = (1 - \alpha)^n \alpha^m \tag{6}$$

where $m+n$ is the overall order of reaction [12,13]. Then we have:

$$\ln \left(\frac{d\alpha}{dt} \right) = \ln A - \frac{E}{RT} + n \ln(1 - \alpha) + m \ln \alpha \tag{7}$$

From Eq. (7):

$$\ln \left[\frac{d(1 - \alpha)}{dt} \right] = \ln A - \frac{E}{RT'} + n \ln \alpha + m \ln(1 - \alpha) \tag{8}$$

Table 4
Order of reaction and frequency factor parameters system

System	$m+n$	$2 \ln A$	Correlation coefficient	$n-m$	Correlation coefficient	n	m	A
A1	1.222	29	0.99613	0.802	0.98058	1.01	0.21	$e^{14.5}$
A2	2.788	39.242	0.99854	0.996	0.97215	1.89	0.90	$e^{19.6}$
A3	1.720	38.662	0.99446	1.057	0.98516	1.39	0.33	$e^{19.33}$
A4	2.202	41.098	0.99423	1.447	0.99398	1.82	0.38	$e^{20.55}$
A5	2.693	43.480	0.97865	1.332	0.97881	2.01	0.68	$e^{21.74}$
A6	1.965	43.023	0.99476	0.974	0.99587	1.47	0.50	$e^{21.51}$
A7	1.432	42.687	0.99847	1.012	0.99438	1.22	0.21	$e^{21.34}$

Eq. (7)+Eq. (8):

$$\ln\left(\frac{d\alpha}{dt}\right) + \frac{E}{RT} + \ln\left[\frac{d(1-\alpha)}{dt}\right] + \frac{E}{RT'}$$

$$= 2\ln A + (m+n)\ln(\alpha - \alpha^2) \tag{9}$$

From the slope and the intercept of the plot of $\ln(d\alpha/dt)+E/RT+\ln[d(1-\alpha)/dt]+E/RT'$ vs. $\ln(\alpha - \alpha^2)$, the values of $m+n$ and $2\ln A$ can be obtained.

Eq. (7)−Eq. (8):

$$\ln\left(\frac{d\alpha}{dt}\right) + \frac{E}{RT} - \ln\left[\frac{d(1-\alpha)}{dt}\right] - \frac{E}{RT'}$$

$$= (n-m)\ln\left[\frac{(1-\alpha)}{\alpha}\right] \tag{10}$$

From the slope of the plot of $\ln(d\alpha/dt)+E/RT-\ln[d(1-\alpha)/dt]-E/RT'$ vs. $\ln[(1-\alpha)/\alpha]$, the value of $n-m$ can be obtained.

The calculated values of E for A1–A7 systems are reported in Table 3, while the values of $m+n$ and A as well as the curing kinetic equations, tabulated in Tables 4 and 5, have been calculated. The results indicated that the values of E, $m+n$ and A of the nano-SiC particles filled systems increase with the increasing nano-SiC particles content. Meanwhile, the addition of the amino silane-coupling agent decreases these parameters. The decrease of the curing kinetic parameters is beneficial to the conduct of curing process and the practical application for the nanocomposite.

The increased values of E for the filled systems also implied that the nano-SiC particles inhibit the curing process. Since the effect of increased concentration of the amino silane coupling agent was equal to the effect of increased EMI-2,4 concentration in the curing system, it is understandable of the decreased values of E when the nano-SiC particles coupled with higher concentration of the amino silane coupling agent.

4. Conclusion

Fractional extent of conversion vs. temperature curves of all the systems considered present the same sigmoidal functional form which is indicative of an autocatalytic kinetics, that is to say, the addition of nano-SiC particles and amino silane coupling agent does not change the cure reaction mechanism.

Comparison the curing process between the filled systems and the pure system, it was found that the addition of the nano-SiC particles contributes to baffle the occurrence of cure reaction. This effect is also manifested in an enhancement of the values of the exothermic peak temperature T_p and the cure reaction activation energy E of the filled systems compared with the corresponding values of the base epoxy resin. Meanwhile, the amino silane coupling agent can decrease slightly the degree of delayed cure reactions caused by the nano-SiC particles, therefore, leading to the decrease of T_p of the filled systems.

The DSC analyses also revealed that the presence of the nano-SiC particles decreases the heat of reaction ΔH, while the amino silane coupling agent increases ΔH.

In this work, the presence of nano-SiC particles prevents from the occurrence of vitrification phenomena, and the amino silane coupling agent promotes the vitrification as the nano-SiC particle contents is above 15 wt% while the amino silane coupling agent preventing from the vitrification as the nano-SiC particle contents is below 15 wt%.

Results also showed that the presence of SiC particles can significantly increase the overall order of reaction $m+n$ and the frequency factor A, besides E, meanwhile, the amino silane coupling agent decreases these three parameters.

Table 5
Curing kinetic equations system

System	Curing kinetic equation
A1	$d\alpha/dt = e^{14.5}e^{(-49.03/RT)}(1-\alpha)^{1.01}\alpha^{0.21}$, $\alpha\varepsilon[0,1]$
A2	$d\alpha/dt = e^{19.6}e^{(-66.32/RT)}(1-\alpha)^{1.89}\alpha^{0.90}$, $\alpha\varepsilon[0,1]$
A3	$d\alpha/dt = e^{19.33}e^{(-67.80/RT)}(1-\alpha)^{1.39}\alpha^{0.33}$, $\alpha\varepsilon[0,1]$
A4	$d\alpha/dt = e^{20.55}e^{(-71.75/RT)}(1-\alpha)^{1.82}\alpha^{0.38}$, $\alpha\varepsilon[0,1]$
A5	$d\alpha/dt = e^{21.74}e^{(-76.29/RT)}(1-\alpha)^{2.01}\alpha^{0.68}$, $\alpha\varepsilon[0,1]$
A6	$d\alpha/dt = e^{21.51}e^{(-68.33/RT)}(1-\alpha)^{1.47}\alpha^{0.50}$, $\alpha\varepsilon[0,1]$
A7	$d\alpha/dt = e^{21.34}e^{(-61.52/RT)}(1-\alpha)^{1.22}\alpha^{0.21}$, $\alpha\varepsilon[0,1]$

References

[1] Yangyang S, Zhuqing Z, Wong CP. IEEE, 9th International symposium and exhibition on advanced packaging materials. Processes Prop Interfaces 2004;9:253–9.

[2] Yangyang S, Zhuqing Z, Kyoung-Sik M, Wong CP. J Polym Sci 2004; 42:3849–58.

[3] Farkas A, Strohm PF. J Appl Polym Sci 1968;12:159.

[4] Heise MS, Martin GC. J Polym Sci 1988;26:153–7.

[5] Heise MS, Martin GC. Macromolecules 1989;22:99.

[6] Duotai Z. China Adhes 1997;6:38–43.

[7] Levenspiel O. Chemical reaction engineering. 2nd ed. New York: Wiley; 1972. p. 56–8.

[8] Akatsuka M, Takezawa Y, Amagi S. Polymer 2001;42:3003–7.

[9] Yangyang S, Zhuqing Z, Wong CP. IEEE, Electric Components Tech Conf 2004;754–60.

[10] Shijian L, Wong CP. IEEE, Trans Components Packaging Tech 2001; 24:38–42.

[11] Ozawa T. Bull Chem Soc Jpn 1965;38:1881.

[12] Wendlandt W.Wm. Thermal analysis. New York: Wiley; 1986. p. 269–84.

[13] Kamal MR, Sourour S. Polym Eng Sci 1973;13:59.